Discrete-Time Fractional-Order Dynamical Networks Minimum-Energy State Estimation

Sarthak Chatterjee, Andrea Alessandretti, Antonio Pedro Aguiar, *Senior Member, IEEE*, and Sérgio Pequito, *Senior Member, IEEE*

***Abstract*—Fractional-order dynamical networks are increasingly being used to model and describe processes demonstrating long-term memory or complex interlaced dependencies among the spatial and temporal components of a wide variety of dynamical networks. Notable examples include networked control systems or neurophysiological networks which are created using electroencephalographic (EEG) or blood-oxygen-level-dependent data. As a result, the estimation of the states of fractional-order dynamical networks poses an important problem. To this effect, this article addresses the problem of minimum-energy state estimation for discrete-time fractional-order dynamical networks, where the state and output equations are affected by an additive noise that is considered to be deterministic, bounded, and unknown. Specifically, we derive the corresponding estimator and show that the resulting estimation error is exponentially input-to-state stable with respect to the disturbances and to a signal that is decreasing with the increase of the accuracy of the adopted approximation model. An illustrative example shows the effectiveness of the proposed method on real-world neurophysiological networks. Our results may significantly contribute to the development of novel neurotechnologies, particularly in the development of state estimation paradigms for neural signals such as EEG, which are often noisy signals known to be affected by artifacts not having any particular stochastic characterization.**

***Index Terms*—Biological networks, cyberphysical systems, decision or estimation theory, other applications.**

Manuscript received 2 August 2021; revised 3 March 2022 and 19 March 2022; accepted 20 March 2022. Date of publication 16 August 2022; date of current version 13 March 2023. This work was supported by the U.S. National Science Foundation under Grant CMMI-1936578 and in part by project RELIABLE (PTDC/EEI-AUT/3522/2020) funded by national funds through FCT/MCTES. Recommended by Associate Editor Adilson E. Motter. *(Corresponding author: Sarthak Chatterjee.)*

Sarthak Chatterjee is with the Department of Electrical, Computer, and Systems Engineering, Rensselaer Polytechnic Institute, Troy, NY 12180 USA (e-mail: sarthak.chatterjee92@gmail.com).

Andrea Alessandretti is with the Hilti Group, Feldkircherstrasse 100, Postfach 333 9494 Schaan, Liechtenstein (e-mail: andrea.alessandretti@gmail.com).

Antonio Pedro Aguiar is with the Department of Electrical and Computer Engineering, Faculty of Engineering, University of Porto, 4200-465 Porto, Portugal (e-mail: pedro.aguiar@fe.up.pt).

Sérgio Pequito is with the Department of Information Technology, Uppsala University, SE 75105 Uppsala, Sweden (e-mail: sergio.pequito@gmail.com).

Digital Object Identifier 10.1109/TCNS.2022.3198832

I. Introduction

In a wide variety of dynamical networks, it is often seen that a Markovian dependence of the current state on only the previous state is insufficient to describe the long-term behavior of the considered systems [1]. This is due to the fact that real-world networks often demonstrate behaviors in which the current system state is dependent on a combination of several past states or the entire gamut of states seen so far in time. Recent works suggest that discrete-time fractional-order dynamical networks (DT-FODNs) evince great success in accurately modeling dynamics that show evidence of nonexponential power-law decay in the dependence of the current state on past states, systems exhibiting long-term memory or fractal properties, or dynamics where there are adaptations in multiple time scales [2], [3], [4], [5], [6]. These networks include biological swarms [7]; networked control systems [8], [9], [10]; and cyber-physical systems [11] to mention a few. Some of these relationships have also been explored in the context of neurophysiological networks constructed from electroencephalographic (EEG), electrocorticographic, or blood-oxygen-level-dependent data [12], [13].

On the other hand, the problem of state estimation entails the retrieval of the internal state of a given network, often from incomplete or partial measurements of the network's inputs and outputs. Solving this problem is of utmost importance, since, in the majority of real-world networks exchanging measurement information with each other, the network's states are often not directly measurable, and a knowledge of the states is needed to, e.g., collectively stabilize the system using state feedback. Given the fundamental nature of the problem, the existence of prior art in the context of state estimation of continuous as well as discrete-time fractional-order systems is no surprise [14], [15], [16], [17], [18], [19], [20], [21], [22].

Nonetheless, in practice, the assumptions in Kalman-like filter formulations can be restrictive and not suitable for some applications, as they assume Gaussian additive process and measurement noises, which implies a uniform prevalence in the power spectrum. In particular, in the case of EEG signals, there is evidence that the former are prone to disturbances that are noncerebral in origin, which are known as artifacts in the neuroscience literature [23]. These artifacts do not follow any particular stochastic characterization. Due to this reason, we propose the design of a minimum-energy estimation (MEE) framework for DT-FODNs, where we assume that the state and output equations are affected by an additive disturbance

and noise, respectively, that is considered to be deterministic, bounded, and unknown. First proposed by Mortensen [24] and later refined by Hijab [25], MEEs produce an estimate of the system state that is the "most consistent" with the dynamics and the measurement updates of the system [26], [27], [28], [29], [30], [31], [32], [33], [34], [35], [36], [37], [38], [39], [40], [41].

To summarize, the main contribution of this article is a MEE procedure to estimate the states of a DT-FODN. In particular, we prove the exponential input-to-state stability of the estimation error when the aforementioned estimator is used to estimate the states of a DT-FODN. We also provide evidence of the efficacy of our approach via a pedagogical example showing the successful estimation of the states of a neurophysiological network constructed using EEG data. Our results provide a structured approach to estimating the states of a DT-FODN in the presence of deterministic and bounded, but unknown disturbances, thus, paving a path for state estimation in neural signals such as EEG, in the presence of noncerebral artifacts.

Notation: The symbols $\mathbb{R}$, $\mathbb{R}^+$, $\mathbb{Z}$, $\mathbb{N}$, and $\mathbb{N}^+$ denote the set of reals, positive reals, integers, non-negative integers, and positive integers, respectively. Additionally, $\mathbb{R}^n$ and $\mathbb{R}^{n\times m}$ represent the set of column vectors of size n and $n \times m$ matrices with real entries and I denotes an identity matrix of appropriate order. For a given square matrix $M \in \mathbb{R}^{n\times n}$, the notation $M \succeq 0$ (respectively, $M \preceq 0$) indicates that the matrix M is positive semidefinite (respectively, negative semidefinite), i.e., $v^\mathsf{T} M v \geq 0$ (respectively, $v^\mathsf{T} M v \leq 0$) for any $v \in \mathbb{R}^n$. Furthermore, we use $M^{-\mathsf{T}}$ to denote the inverse of M^T. We also write $A \succeq B$ and $A \preceq B$ to mean that the matrix $A - B$ is positive semidefinite and negative semidefinite, respectively. The Euclidean norm is denoted by $\|\cdot\|$.

II. Problem Formulation

In this section, we introduce DT-FODN and formulate the minimum-energy state estimation problem for DT-FODN.

A. Continuous-Time and DT-FODNs

The concept of fractional-order dynamical networks arises from the concept of a fractional-order derivative. There are two commonly used (and equivalent) definitions of a fractional-order derivative, the Caputo and the Riemann–Liouville definitions [42]. Caputo's definition of a fractional derivative is as follows:

$$\Delta^{\alpha_i}\sigma(t) = \frac{1}{\Gamma(m-\alpha_i)}\int_0^t \frac{\Delta^m \sigma(\tau)}{(t-\tau)^{\alpha_i+1-m}}\,\mathrm{d}\tau \tag{1}$$

with

$$\Gamma(\alpha_i) = \int_0^\infty e^{-\tau}\tau^{\alpha_i-1}\,\mathrm{d}\tau \tag{2}$$

where $\Gamma(\alpha_i)$ denotes the Gamma function [43], $\alpha_i \in \mathbb{R}^+, i \in \{1,\ldots,n\}$ is the fractional exponent, and $m \in \mathbb{Z}$ is the first integer not less than α_i for all i, i.e., $m = \lceil \alpha_i \rceil$ for all i. With the above ingredients, a continuous-time fractional-order dynamical network is given by

$$\Delta^\alpha x(t) = Ax(t) + Bu(t), \tag{3a}$$

$$y(t) = Cx(t) + Du(t) \tag{3b}$$

with $\alpha = [\alpha_1, \ldots, \alpha_n]^\mathsf{T}$.

Consider a left-bounded sequence $\{x[k]\}_{k\in\mathbb{Z}}$ over k, i.e., with $\limsup_{k\to-\infty}\|x[k]\| < \infty$. Then, for any $\alpha \in \mathbb{R}^+$, the Grünwald–Letnikov fractional-order difference is defined as

$$\Delta^\alpha x[k] := \sum_{j=0}^{\infty} c_j^\alpha x[k-j], \quad c_j^\alpha = (-1)^j\binom{\alpha}{j},$$

$$\binom{\alpha}{j} = \begin{cases} 1 & \text{if } j = 0, \\ \prod_{i=0}^{j-1}\frac{\alpha-i}{i+1} = \frac{\Gamma(\alpha+1)}{\Gamma(j+1)\Gamma(\alpha-j+1)} & \text{if } j > 0 \end{cases} \tag{4}$$

for all $j \in \mathbb{N}$. The summation in (4) is well defined from the uniform boundedness of the sequence $\{x[k]\}_{k\in\mathbb{Z}}$ and the fact that $|c_j^\alpha| \leq \frac{\alpha^j}{j!}$, which implies that the sequence $\{c_j^\alpha\}_{j\in\mathbb{N}}$ is absolutely summable for any $\alpha \in \mathbb{R}^+$ [44], [45].

With the above ingredients, a *DT-FODN with additive disturbance* can be described, respectively, by the state evolution and output equations

$$\sum_{i=1}^{l} A_i \Delta^{a_i} x[k+1] = \sum_{i=1}^{r} B_i \Delta^{b_i} u[k] + \sum_{i=1}^{s} G_i \Delta^{g_i} w[k], \tag{5a}$$

$$z[k] = C_k' x[k] + v'[k] \tag{5b}$$

with the variables $x[k] \in \mathbb{R}^n$, $u[k] \in \mathbb{R}^m$, and $w[k] \in \mathbb{R}^p$ denoting the *state*, *input*, and *disturbance* vectors at time step $k \in \mathbb{N}$, respectively. The scalars $a_i \in \mathbb{R}^+$ with $1 \leq i \leq l$, $b_i \in \mathbb{R}^+$ with $1 \leq i \leq r$, and $g_i \in \mathbb{R}^+$ with $1 \leq i \leq s$ are the *fractional-order coefficients* corresponding, respectively, to the state, the input, and the disturbance. The vectors $z[k], v'[k] \in \mathbb{R}^q$ denote the *output* and *measurement disturbance* at time step $k \in \mathbb{N}$, respectively.

We assume that the (unknown but deterministic) disturbance vectors are bounded as

$$\|w[k]\| \leq b_w, \|v'[k]\| \leq b_{v'},\ k \in \mathbb{N} \tag{6}$$

for some scalars $b_w, b_{v'} \in \mathbb{R}^+$. Notice that the assumption that the disturbance vectors are deterministic, bounded, unknown, and not possessing any particular stochastic characterization, is distinctly different from the assumptions one makes in deriving the Kalman filter, in which case, the disturbances are assumed to be additive, white, and Gaussian [46], which would not be satisfied when we are dealing with a setting characterized by the absence of uniform prevalence of frequency components in the power spectral density of the disturbances.

We also assume that the control input $u[k]$ is known for all time steps $k \in \mathbb{N}$. We denote by $x[0] = x(0)$ the initial condition of the state at time $k = 0$. In the computation of the fractional-order difference, we assume that the system is *causal*, i.e., the state, input, and disturbances are all considered to be zero before the initial time (i.e., $x[k] = 0$, $u[k] = 0$, and $w[k] = 0$ for all $k < 0$).

In addition, the matrices $A_i \in \mathbb{R}^{n\times n}, 1 \leq i \leq l$ denote the (possibly time-varying) spatial dependencies between the state variables at different time lags, the matrices $B_i \in \mathbb{R}^{n\times m}, 1 \leq i \leq r$ denote the dependency of which (known) input variables

are being actuated at different time steps, and the matrices $G_i \in \mathbb{R}^{n\times p}, 1 \leq i \leq s$ are the disturbances acting as (unknown) inputs into the system at a particular time instant.

Given that we have determined the nature of the deterministic but unknown process and output uncertainties, we can now focus on trying to minimize the impact of these uncertainties, as well as the uncertainty with respect to the unknown initial state $x[0]$. Henceforth, we will focus on trying to minimize the objective function $\mathcal{J}(x[0], \{w[i]\}_{i=0}^{N-1}, \{v'[j]\}_{j=1}^{N})$, for some $N \in \mathbb{N}$, subject to the evolution of the state and output trajectories given by (5a) and (5b). There are a wide variety of choices we can consider for the objective function $\mathcal{J}(\cdot,\cdot,\cdot)$, but from a computational perspective, and considering an association with the process of minimizing an energy functional, we take the objective function to consist of quadratic terms with respect to the components pertaining to the process and output disturbances as well as the uncertainty pertaining to the initial state.

With the above ingredients, we seek to solve the following problem in this article.

Problem 1: Consider the quadratic weighted least-squares objective function

$$\mathcal{J}\left(x[0], \{w[i]\}_{i=0}^{N-1}, \{v'[j]\}_{j=1}^{N}\right) = \sum_{i=0}^{N-1} w[i]^{\mathsf{T}} Q_i^{-1} w[i] + \sum_{j=1}^{N} v'[j]^{\mathsf{T}} R_j^{-1} v'[j] + (x[0]-\hat{x}_0)^{\mathsf{T}} P_0^{-1} (x[0]-\hat{x}_0) \quad (7)$$

subject to the constraints

$$\sum_{i=1}^{l} A_i \Delta^{a_i} x[k+1] = \sum_{i=1}^{r} B_i \Delta^{b_i} u[k] + \sum_{i=1}^{s} G_i \Delta^{g_i} w[k] \quad (8a)$$

and

$$z[k] = C_k' x[k] + v'[k] \quad (8b)$$

for some $N \in \mathbb{N}$, with the weighting matrices Q_i $(0 \leq i \leq N-1)$, R_j $(1 \leq j \leq N)$, and P_0 chosen to be symmetric and positive definite, and $\hat{x}_0$ chosen to be the *a priori* estimate of the system's initial state. The MEE procedure seeks to solve the following optimization problem:

$$\begin{aligned} \underset{\{x[k]\}_{k=0}^{N}, \{w[i]\}_{i=0}^{N-1}, \{v'[j]\}_{j=1}^{N}}{\text{minimize}} \quad & \mathcal{J}\left(x[0], \{w[i]\}_{i=0}^{N-1}, \{v'[j]\}_{j=1}^{N}\right) \\ \text{subject to} \quad & \text{(8a) and (8b)} \end{aligned} \quad (9)$$

for some $N \in \mathbb{N}$.

Additionally, we consider the following mild technical assumption to hold.

Assumption 1: The matrix $\sum_{i=1}^{l} A_i$ is invertible.

III. MEE for Discrete-Time Fractional-Order Dynamical Networks

In order to derive the solution to Problem 1, we will first start with some alternative formulations of the DT-FODN and relevant definitions that will be used in the sequel. Then, we present the solution in Section III-A and in Section III-B we provide some additional properties of the derived solution, i.e., the exponential input-to-state stability of the estimation error. In Section III-D, we present a practical discussion of the results obtained in the context of DT-FODN. All proofs are relegated to the Appendix.

We start by considering a truncation of the last $\mathfrak{v}$ temporal components of (5a), which we will refer to as the $\mathfrak{v}$-approximation for the DT-FODN. That being said, we note that using Assumption 1, the DT-FODN model in (5a) can be equivalently written as

$$x[k+1] = \sum_{j=1}^{\infty} \check{A}_j x[k-j+1] + \sum_{j=0}^{\infty} \check{B}_j u[k-j] + \sum_{j=0}^{\infty} \check{G}_j w[k-j] \quad (10)$$

where $\check{A}_j = -\hat{A}_0^{-1}\hat{A}_j$, $\check{B}_j = \hat{A}_0^{-1}\hat{B}_j$, and $\check{G}_j = \hat{A}_0^{-1}\hat{G}_j$ with $\hat{A}_j = \sum_{i=1}^{l} A_i c_j^{a_i}$, $\hat{B}_j = \sum_{i=1}^{r} B_i c_j^{b_i}$, and $\hat{G}_j = \sum_{i=1}^{s} G_i c_j^{g_i}$. Notice that if the network is intrinsically linear time-invariant (LTI), then, a suitable choice of zero fractional exponents would seamlessly model the LTI dynamics. Nonetheless, we obtain an infinite-dimensional linear system due to the presence of the infinite sum in (10). However, the entirety of the dynamics admits a compact abstraction using just the parameters a_i and A_i, $1 \leq i \leq l$. Furthermore, for any positive integer $\mathfrak{v} \in \mathbb{N}^+$, the DT-FODN model in (5a) can be recast as

$$\tilde{x}[k+1] = \tilde{A}_{\mathfrak{v}} \tilde{x}[k] + \tilde{B}_{\mathfrak{v}} u[k] + \tilde{G}_{\mathfrak{v}} r[k], \qquad \tilde{x}[0] = \tilde{x}_0, \quad (11a)$$

$$y[k+1] = C_{k+1} \tilde{x}[k+1] + v[k+1] \quad (11b)$$

where

$$r[k] = \sum_{j=\mathfrak{v}+1}^{\infty} \check{A}_j x[k-j+1] + \sum_{j=\mathfrak{v}+1}^{\infty} \check{B}_j u[k-j] + \sum_{j=0}^{\infty} \check{G}_j w[k-j] \quad (12)$$

with the augmented state vector $\tilde{x}[k] = [x[k]^{\mathsf{T}}, \ldots, x[k-\mathfrak{v}+1]^{\mathsf{T}}, u[k-1]^{\mathsf{T}}, \ldots, u[k-\mathfrak{v}]^{\mathsf{T}}]^{\mathsf{T}} \in \mathbb{R}^{\mathfrak{v}\times(n+m)}$, and appropriate matrices $\tilde{A}_{\mathfrak{v}}$, $\tilde{B}_{\mathfrak{v}}$, and $\tilde{G}_{\mathfrak{v}}$, where $\tilde{x}_0 = [x_0^{\mathsf{T}}, 0, \ldots, 0]^{\mathsf{T}}$ denotes the initial condition. $y[k]$ represents the output and the matrix C_k represents the scaling between the states and the outputs, with $\mathfrak{v}$ representing the temporal memory dependency, the dependency being retained for the last $\mathfrak{v}$ temporal components. The matrices $\tilde{A}_{\mathfrak{v}}$ and $\tilde{B}_{\mathfrak{v}}$ are formed using the terms $\{\check{A}_j\}_{1\leq j\leq \mathfrak{v}}$ and $\{\check{B}_j\}_{1\leq j\leq \mathfrak{v}}$, while the remaining terms $\{\check{G}_j\}_{1\leq j<\infty}$ and the state and input components not included in $\tilde{x}[k]$ are absorbed into the term $\tilde{G}_{\mathfrak{v}} r[k]$. Furthermore, we refer to (11a) as the $\mathfrak{v}$-*approximation* of the DT-FODN presented in (5a).

A. Minimum-Energy Estimator

First, let us consider the quadratic weighted least-squares objective function

$$\mathcal{J}\left(\tilde{x}[0], \{r[i]\}_{i=0}^{N-1}, \{v[j]\}_{j=1}^{N}\right) = \sum_{i=0}^{N-1} r[i]^{\mathsf{T}} Q_i^{-1} r[i]$$

$$+\sum_{j=1}^{N} v[j]^{\mathsf{T}} R_j^{-1} v[j] + (\tilde{x}[0]-\hat{x}_0)^{\mathsf{T}} P_0^{-1} (\tilde{x}[0]-\hat{x}_0) \quad (13)$$

subject to the constraints

$$\bar{x}[k+1] = \tilde{A}_{\mathfrak{v}} \bar{x}[k] + \tilde{B}_{\mathfrak{v}} u[k] + \tilde{G}_{\mathfrak{v}} \bar{r}[k], \quad (14a)$$

$$y[k+1] = C_{k+1} \bar{x}[k+1] + \bar{v}[k+1] \quad (14b)$$

for some $N \in \mathbb{N}$. The weighting matrices Q_i $(0 \leq i \leq N-1)$ and R_j $(1 \leq j \leq N)$ are chosen to be symmetric and positive definite. The term $\hat{x}_0$ denotes the a priori estimate of the (unknown) initial state of the system, with the matrix P_0 being symmetric and positive definite.

Subsequently, to construct a minimum-energy estimator for the system (11), we then consider the weighted least-squares optimization problem

$$\begin{aligned} &\underset{\{\bar{x}[k]\}_{k=0}^{N}, \{\bar{r}[i]\}_{i=0}^{N-1}, \{\bar{v}[j]\}_{j=1}^{N}}{\text{minimize}} && \mathcal{J}\left(\tilde{x}[0], \{r[i]\}_{i=0}^{N-1}, \{v[j]\}_{j=1}^{N}\right) \\ &\text{subject to} && (14a) \text{ and } (14b) \end{aligned} \quad (15)$$

for some $N \in \mathbb{N}$. The following theorem then certifies the solution of the MEE problem posed in (15).

Theorem 1: Denote by $\hat{x}[k]$ the state vector that corresponds to the solution of the optimization problem (15). Then, $\hat{x}[k]$ satisfies the recursion

$$\begin{aligned} \hat{x}[k+1] &= \tilde{A}_{\mathfrak{v}} \hat{x}[k] + \tilde{B}_{\mathfrak{v}} u[k] + K_{k+1} \left(y[k+1]\right. \\ &\left. - C_{k+1}\left(\tilde{A}_{\mathfrak{v}} \hat{x}[k] + \tilde{B}_{\mathfrak{v}} u[k]\right)\right), \quad 0 \leq k \leq N-1 \end{aligned} \quad (16)$$

with initial conditions specified for $\hat{x}_0$ and $\{u[j]\}_{j=0}^{k}$, and with the update equations

$$K_{k+1} = M_{k+1} C_{k+1}^{\mathsf{T}} \left(C_{k+1} M_{k+1} C_{k+1}^{\mathsf{T}} + R_{k+1}\right)^{-1}, \quad (17a)$$

$$M_{k+1} = \tilde{A}_{\mathfrak{v}} P_k \tilde{A}_{\mathfrak{v}}^{\mathsf{T}} + \tilde{G}_{\mathfrak{v}} Q_k \tilde{G}_{\mathfrak{v}}^{\mathsf{T}} \quad (17b)$$

and

$$\begin{aligned} P_{k+1} &= (I - K_{k+1} C_{k+1}) M_{k+1} (I - K_{k+1} C_{k+1})^{\mathsf{T}} \\ &+ K_{k+1} R_{k+1} K_{k+1}^{\mathsf{T}} = (I - K_{k+1} C_{k+1}) M_{k+1} \end{aligned} \quad (17c)$$

with symmetric and positive definite P_0.

Proof: The proof of Theorem 1 follows directly from [28], Ths. 2.3 and 2.4], which, in turn, follow from formalizing the properties of the discrete-time algebraic Riccati equation (DARE) [47] – see, for instance, in [28], Lemmas 4.3–4.7, Proposition 4.8]. Broadly speaking, the key steps of the proof can be structured as follows. We first consider a single-stage state transition of the system in (14) and, then, sequentially, course through the remaining state transitions. Then, the iterative closed-form recursions in (16) and (17) are obtained using the principle of feedback invariance [48] and the minimum-energy estimator for discrete-time LTI systems [28], since the $\mathfrak{v}$-approximated DT-FODN in (11a) fits the latter description.■

In Theorem 1, the dynamics of the recursion in (16) (with the initial conditions on $\hat{x}_0$ and the values of $\{u[j]\}_{j=0}^{k}$ being known) along with the update equations (17) together solve Problem 1 completely. It is interesting to note here that the output term $y[k+1]$ presented in (14b) and (16) is the output of the $\mathfrak{v}$-approximated system (11), which, in turn, is simply a subset of the outputs $z[k+1]$ obtained from (5b), truncated $\mathfrak{v}$ time steps in the past, provided $v[k]$ and C_k are formed from the appropriate blocks of $v'[k]$ and C_k' for all $k \in \mathbb{N}$.

In what follows, we show that given the $\mathfrak{v}$-approximation outlined in (11a), the evolution of the Lyapunov equation admits a solution over time, by establishing the exponential input-to-state stability of the estimation error.

B. Exponential Input-to-State Stability of the Estimation Error

In order to prove the exponential input-to-state stability of the MEE error, we need to consider the following mild technical assumptions:

Assumption 2: There exist constants $\underline{\alpha}, \overline{\alpha}, \beta, \gamma \in \mathbb{R}^+$ such that

$$\underline{\alpha} I \preceq \tilde{A}_{\mathfrak{v}} \tilde{A}_{\mathfrak{v}}^{\mathsf{T}} \preceq \overline{\alpha} I, \quad \tilde{G}_{\mathfrak{v}} \tilde{G}_{\mathfrak{v}}^{\mathsf{T}} \preceq \beta I, \text{ and } C_k^{\mathsf{T}} C_k \preceq \gamma I \quad (18)$$

for all $k \in \mathbb{N}$.

First, notice that the *state transition matrix* for the dynamics in (11a) is given by

$$\Phi(k, k_0) = \tilde{A}_{\mathfrak{v}}^{(k-k_0)}, \quad \text{with} \quad \Phi(k_0, k_0) = I \quad (19)$$

for all $k \geq k_0 \geq 0$. We also consider the *discrete-time controllability Gramian* associated with the dynamics (11a) described by

$$W_c(k, k_0) = \sum_{i=k_0}^{k-1} \Phi(k, i+1) \tilde{G}_{\mathfrak{v}} \tilde{G}_{\mathfrak{v}}^{\mathsf{T}} \Phi^{\mathsf{T}}(k, i+1) \quad (20)$$

and the *discrete-time observability Gramian* associated with (11a) to be

$$W_o(k, k_0) = \sum_{i=k_0+1}^{k} \Phi^{\mathsf{T}}(i, k_0) C_i^{\mathsf{T}} C_i \Phi(i, k_0) \quad (21)$$

for $k \geq k_0 \geq 0$. We also make the following assumptions regarding *complete uniform controllability* and *complete uniform observability* of the $\mathfrak{v}$-approximated system in (11a).

Assumption 3: The $\mathfrak{v}$-approximated system (11a) is completely uniformly controllable, i.e., there exist constants $\delta \in \mathbb{R}^+$ and $N_c \in \mathbb{N}^+$ such that

$$W_c(k + N_c, k) \succeq \delta I \quad (22)$$

for all $k \geq 0$.

Assumption 4: The $\mathfrak{v}$-approximated system (11a) is completely uniformly observable, i.e., there exist constants $\varepsilon \in \mathbb{R}^+$ and $N_o \in \mathbb{N}^+$ such that

$$W_o(k + N_o, k) \succeq \varepsilon \Phi^{\mathsf{T}}(k + N_o, k) \Phi(k + N_o, k) \quad (23)$$

for all $k \geq 0$.

Next, we also present an assumption certifying lower and upper bounds on the weight matrices Q_k and R_{k+1} in (13).

Assumption 5: Without loss of generality, we assume that the weight matrices Q_k and R_{k+1} satisfy

$$\underline{\vartheta} I \preceq Q_k \preceq \overline{\vartheta} I \quad \text{and} \quad \underline{\rho} I \preceq R_{k+1} \preceq \overline{\rho} I \quad (24)$$

for all $k \geq 0$ and constants $\underline{\vartheta}, \overline{\vartheta}, \underline{\rho}, \overline{\rho} \in \mathbb{R}^+$.

1) Bounds on the Covariance Matrix P_k: In this section, we establish lower and upper bounds for the matrix P_k, which will be required in Section III-B2, where we use an approach using Lyapunov functions in order to show that the estimation error is exponentially input-to-state stable.

Lemma 1: Given Assumptions 2 and 3 and the constant $\underline{\pi} \in \mathbb{R}^+$, we have that

$$P_k \succeq \underline{\pi}(N_c) I \tag{25}$$

holds for all $k \geq N_c$.

Lemma 2: Given Assumptions 2 and 4 and the constant $\overline{\pi} \in \mathbb{R}^+$, we have that

$$P_k \preceq \overline{\pi}(N_o) I \tag{26}$$

holds for all $k \geq N_o$.

2) Exponential Input-to-State Stability of the Estimation Error: We start with the MEE error $e[k]$, given by

$$e[k] = \hat{x}[k] - \tilde{x}[k]. \tag{27}$$

Next, we certify that the estimation error associated with the MEE process is exponentially input-to-state stable.

Theorem 2: Under Assumptions 2, 3, and 4, there exist constants $\sigma, \tau, \chi, \psi \in \mathbb{R}^+$ with $\tau < 1$ such that the estimation error $e[k]$ satisfies

$$\|e[k]\| \leq \max \left\{ \sigma \tau^{k-k_0} \|e[k_0]\|, \ \chi \max_{k_o \leq i \leq k-1} \|r[i]\|, \right.$$
$$\left. \psi \max_{k_o \leq j \leq k-1} \|v[j+1]\| \right\} \tag{28}$$

for all $k \geq k_0 \geq \max\{N_c, N_o\}$.

Note that the above result provides us with theoretical guarantees to obtain an estimate of the system state that is the most consistent with the dynamics and the measurement updates of the system in the context of DT-FODNs. In particular, in the context of designing novel neurotechnologies, we will see an application of this result in estimating the states of real-life biological signals modeled using DT-FODNs, such as EEG signals, presented in Section III-D. Furthermore, the above input-to-state stability result has important consequences in the study of complex interconnections of networked systems in which our minimum-energy estimator framework constitutes one particular block in a larger chain of blocks—see, for instance [49] and [50].

C. Discussion

It is interesting to note that the bound on the estimation error $e[k]$ in (28) actually depends on $\|r[i]\|$, where $k_0 \leq i \leq k-1$ for all $i \in \mathbb{N}$. In fact, a distinguishing feature of DT-FODN is the presence of a finite nonzero disturbance term in the input-to-state stability bound of the tracking error when tracking a state other than the origin. This disturbance is dependent on the upper bounds on the nonzero reference state being tracked as well as the input. While the linearity of the Grünwald–Letnikov fractional-order difference operator allows one to mitigate this issue in the case of tracking a nonzero exogenous state by a suitable change of state and input coordinates, this approach is not one we can pursue in this article, since the state we wish to estimate is unknown. However, it can be shown that as the value of $\mathfrak{v}$ in the $\mathfrak{v}$-approximation increases, the upper bound associated with $\|r[i]\|$ decreases drastically since the $\mathfrak{v}$-approximation gives us progressively better representations of the unapproximated system. This further implies that $\|r[i]\|$ in (28) stays bounded, with progressively smaller upper bounds associated with $\|r[i]\|$ (and hence, $\|e[k]\|$) with increasing $\mathfrak{v}$.

Last, the estimation error associated with the MEE process in (27) is defined in terms of the state of the $\mathfrak{v}$-approximated system $\tilde{x}[k]$. In reality, as detailed above, with larger values of $\mathfrak{v}$, the $\mathfrak{v}$-approximated system approaches the real network dynamics, and, thus, we obtain an expression for the estimation error with respect to the real system in the limiting case, where the input-to-state stability bound presented in Theorem 2 holds.

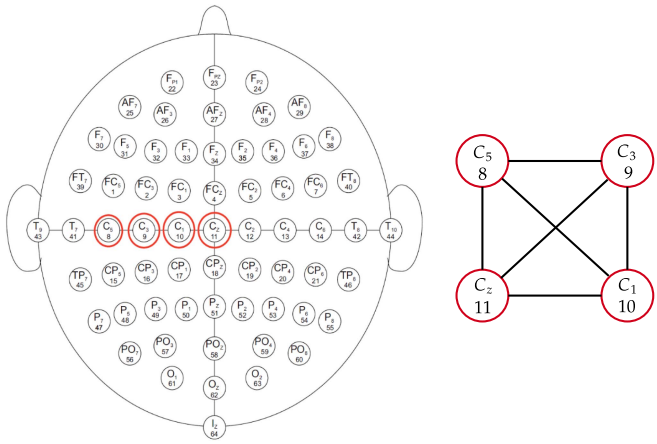

Fig. 1. Distribution of the sensors for the measurement of EEG data is shown on the left. The channel labels are shown along with their corresponding numbers and the selected channels over the motor cortex are shown in red. The corresponding network formed by the EEG sensors is shown on the right.

D. Illustrative Example

In this section, we consider the performance of the MEE paradigm on real-world neurophysiological networks considering EEG data. Specifically, we use 150 noisy measurements taken from 4 channels of a 64-channel EEG signal which records the brain activity of subjects, as shown in Fig. 1. The subjects were asked to perform a variety of motor and imagery tasks, and the specific choice of the 4 channels was dictated due to them being positioned over the motor cortex of the brain, and, therefore, enabling us to predict motor actions such as the movement of the hands and feet. The data were collected using the BCI2000 system with a sampling rate of 160 Hz [51], [52].

The spatial and temporal parameter components of the DT-FODN assumed to model the original EEG data were identified using the methods described in [53]. The identification process is data driven and is done for the overall DT-FODN. The process to identify the spatial and temporal parameters of the DT-FODN is sequential, with a wavelet-like approach

TABLE I
MEAN ± STANDARD DEVIATION FOR THE ESTIMATION ERROR OF EACH CHANNEL FOR DIFFERENT VALUES OF THE TEMPORAL MEMORY DEPENDENCY PARAMETER $\mathfrak{v}$

	Channel 1	Channel 2	Channel 3	Channel 4
$\mathfrak{v} = 2$	0.1177 ± 1.1378	-0.0243 ± 1.2085	0.1122 ± 1.1647	1.0128 ± 2.0140
$\mathfrak{v} = 10$	-0.0136 ± 1.1966	-0.0442 ± 1.2230	0.0622 ± 1.1795	0.3512 ± 1.2236
$\mathfrak{v} = 20$	0.0308 ± 1.3191	0.0630 ± 1.2944	0.1144 ± 1.3075	-0.0539 ± 1.5305

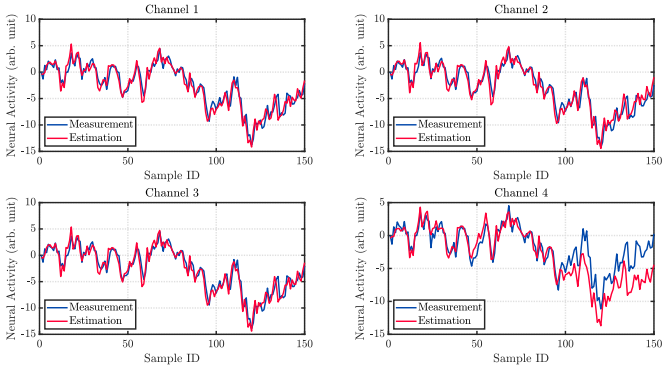

Fig. 2. Comparison between the measured output of the $\mathfrak{v}$-augmented system (with $\mathfrak{v} = 2$) versus the estimated output of a minimum-energy estimator implemented on the same, in the presence of process and measurement noises for 4 channels of a 64-channel EEG signal.

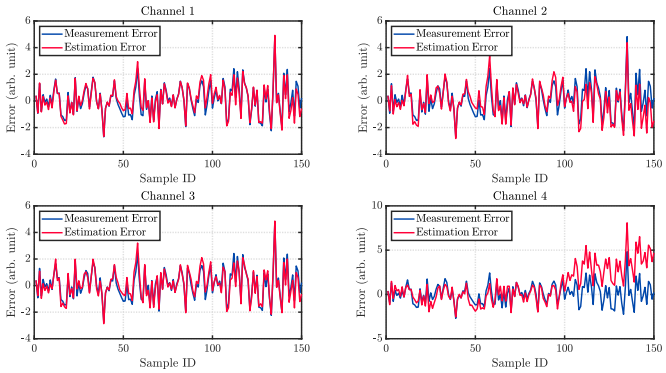

Fig. 3. Comparison between the measurement error of the $\mathfrak{v}$-augmented system (with $\mathfrak{v} = 2$) versus the estimation error of a minimum-energy estimator implemented on the same, in the presence of process and measurement noises for 4 channels of a 64-channel EEG signal.

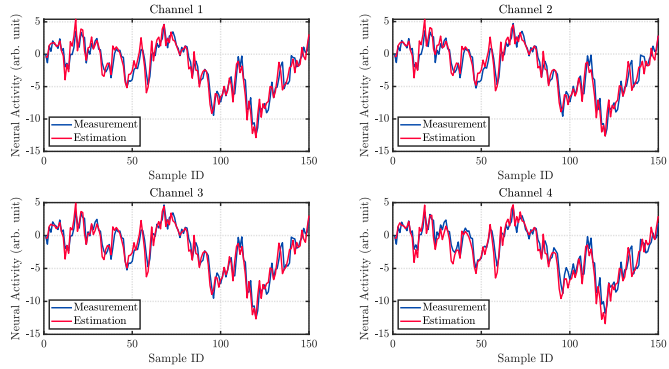

Fig. 4. Comparison between the measured output of the $\mathfrak{v}$-augmented system (with $\mathfrak{v} = 10$) versus the estimated output of a minimum-energy estimator implemented on the same, in the presence of process and measurement noises for 4 channels of a 64-channel EEG signal.

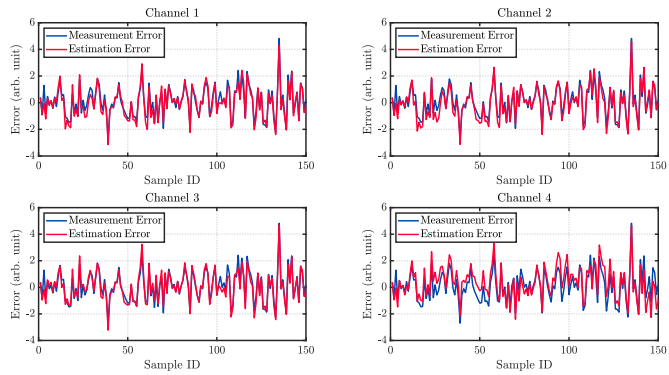

Fig. 5. Comparison between the measurement error of the $\mathfrak{v}$-augmented system (with $\mathfrak{v} = 10$) versus the estimation error of a minimum-energy estimator implemented on the same, in the presence of process and measurement noises for 4 channels of a 64-channel EEG signal.

being used to estimate the temporal parameters, followed by least squares to estimate the spatial parameters. It is relevant to mention here that although this method has demonstrated good results in practice, the identification of fractional-order systems remains an underexplored area in general. Nonetheless, from an analytical perspective it is possible to perform a bilevel iterative scheme to estimate the spatial and temporal parameters of a fractional-order system – see details in [54]. Using the aforementioned approach, the fractional-order coefficients are identified to be $a = [0.9211, 0.9655, 0.9620, 0.8821]^{\mathsf{T}}$. The matrices $B_i = \begin{bmatrix} 1 & 1 & 1 & 1 \end{bmatrix}^{\mathsf{T}}$ for all i.

The results of our approach, considering different values of $\mathfrak{v}$, are shown in Figs. 2 and 3 (for $\mathfrak{v} = 2$), Figs. 4 and 5 (for $\mathfrak{v} = 10$), and Figs. 6 and 7 (for $\mathfrak{v} = 20$), which show, respectively (for each value of $\mathfrak{v}$), the comparison between the measured output of the network with noise and the estimated response obtained from the minimum-energy estimator, and also the juxtaposition of the measurement error and the estimation error of the MEE process. Additionally, we also present in Table I the means and standard deviations for the estimation error for each channel for various values of the temporal dependency parameter $\mathfrak{v}$. We find that the minimum-energy estimator is successfully able to estimate the states in the presence of noise in both the dynamics and the measurement processes.

We also note from the Figs. 2 and 3 that when $\mathfrak{v} = 2$, we get comparatively larger estimation errors associated with the last 50 or so samples of Channel 4, and that this behavior can be mitigated by increasing the value of $\mathfrak{v}$, e.g., by choosing $\mathfrak{v} = 10$

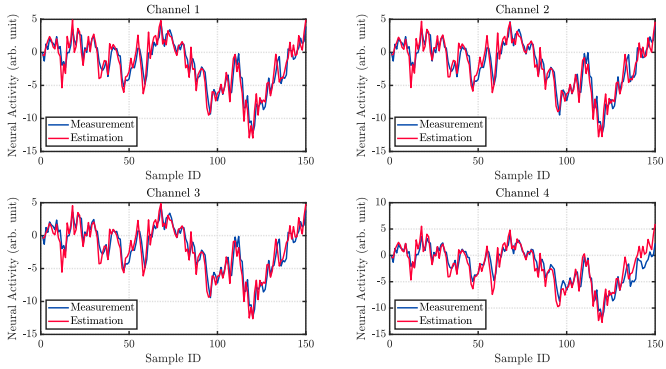

Fig. 6. Comparison between the measured output of the $\mathfrak{v}$-augmented system (with $\mathfrak{v} = 20$) versus the estimated output of a minimum-energy estimator implemented on the same, in the presence of process and measurement noises for 4 channels of a 64-channel EEG signal.

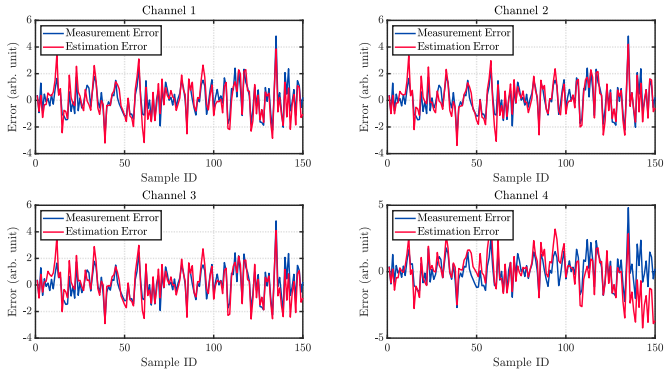

Fig. 7. Comparison between the measurement error of the $\mathfrak{v}$-augmented system (with $\mathfrak{v} = 20$) versus the estimation error of a minimum-energy estimator implemented on the same, in the presence of process and measurement noises for 4 channels of a 64-channel EEG signal.

or $\mathfrak{v} = 20$. This is in line with the discussion in Section III-C, and choosing a larger value of $\mathfrak{v}$ can always, in practice, provide us with better estimation performances, as seen from this example.

IV. Conclusion

In this article, we introduced minimum-energy state estimation for DT-FODNs. In particular, the aforementioned minimum-energy estimator is capable of providing an estimate of the unknown states of a DT-FODN while assuming that the associated process and measurement noises are deterministic, bounded, and unknown in nature. We proved that the MEE error is exponentially input-to-state stable and illustrated its performance on real-world neurophysiological EEG networks, thus, providing a general framework to estimate the states of neural data modeled by DT-FODNs.

Future work will focus on the construction of a resilient and attack-resistant version of the minimum-energy estimator, to take into consideration adversarial attacks or artifacts associated with the measurement process, since, the former approach is consistent with the fact that adversarial attacks on sensors often do not follow any particular dynamical or stochastic characterization.

In addition, it is also important to emphasize the observation that although the estimation accuracy increases with increasing values of the temporal memory dependency $\mathfrak{v}$, it only does so up to a certain value. Further increasing $\mathfrak{v}$ beyond that value leads to no further gains when it comes to the results, thus preventing us from the hassles of dealing with infinite memory. Nonetheless, it is important to emphasize that better understanding the relationship between the dimensions of the state space and the specific values of the fractional coefficients may very well change the value of $\mathfrak{v}$ that leads to good results. The precise nature of this relationship will be the subject of future work.

Appendix

Proof of Lemma 1 Suppose L_{k+1} is an arbitrary matrix. We can write

$$\left(P_{k+1} + L_{k+1}L_{k+1}^{\mathsf{T}}\right)^{-1} = \left(\left(M_{k+1}^{-1} + C_{k+1}^{\mathsf{T}}R_{k+1}^{-1}C_{k+1}\right)^{-1} + L_{k+1}L_{k+1}^{\mathsf{T}}\right)^{-1} \tag{29}$$

where we use the equation

$$P_{k+1}^{-1} = M_{k+1}^{-1} + C_{k+1}^{\mathsf{T}}R_{k+1}^{-1}C_{k+1} \tag{30}$$

which can be obtained from (17c) using the Woodbury identity [55], eq. (157)]. Notice that the invertibility of P_k and M_{k+1} for any $k \geq 0$ is a consequence of (17), Assumptions 2 and 5, and the fact that P_0 is positive definite.

Subsequently, using the bounds in Assumptions 2 and 5, and defining $\beta_1 = \frac{\gamma}{\underline{\rho}}$, we have

$$\begin{aligned}
&\left(P_{k+1} + L_{k+1}L_{k+1}^{\mathsf{T}}\right)^{-1} \\
&\preceq \left(\left(M_{k+1}^{-1} + \beta_1 I\right)^{-1} + L_{k+1}L_{k+1}^{\mathsf{T}}\right)^{-1} \\
&\overset{(\dagger)}{=} \left(\frac{1}{\beta_1}I - \frac{1}{\beta_1^2}\left(M_{k+1} + \frac{1}{\beta_1}I\right)^{-1} + L_{k+1}L_{k+1}^{\mathsf{T}}\right)^{-1} \\
&\overset{(\ddagger)}{=} \frac{1}{\beta_1^2}\left(\frac{1}{\beta_1}I + L_{k+1}L_{k+1}^{\mathsf{T}}\right)^{-1} \\
&\times \left(M_{k+1} + \frac{1}{\beta_1}I - \frac{1}{\beta_1^2}\left(\frac{1}{\beta_1}I + L_{k+1}L_{k+1}^{\mathsf{T}}\right)^{-1}\right)^{-1} \\
&\times \left(\frac{1}{\beta_1}I + L_{k+1}L_{k+1}^{\mathsf{T}}\right)^{-1} + \left(\frac{1}{\beta_1}I + L_{k+1}L_{k+1}^{\mathsf{T}}\right)^{-1} \\
&\overset{(\diamond)}{=} \frac{1}{\beta_1^2}\left(\beta_1 I - \beta_1^2 L_{k+1}\left(I + \beta_1 L_{k+1}^{\mathsf{T}}L_{k+1}\right)^{-1}L_{k+1}^{\mathsf{T}}\right) \\
&\times \left(M_{k+1} + L_{k+1}\left(I + \beta_1 L_{k+1}^{\mathsf{T}}L_{k+1}\right)^{-1}L_{k+1}^{\mathsf{T}}\right)^{-1} \\
&\times \left(\beta_1 I - \beta_1^2 L_{k+1}\left(I + \beta_1 L_{k+1}^{\mathsf{T}}L_{k+1}\right)^{-1}L_{k+1}^{\mathsf{T}}\right) + \beta_1 I \\
&- \beta_1^2 L_{k+1}\left(I + \beta_1 L_{k+1}^{\mathsf{T}}L_{k+1}\right)^{-1}L_{k+1}^{\mathsf{T}}
\end{aligned}$$

$$\overset{(\diamond)}{\preceq} 2\beta_1^2 L_{k+1}\left(I+\beta_1 L_{k+1}^{\mathsf{T}}L_{k+1}\right)^{-1}L_{k+1}^{\mathsf{T}} \times\left(M_{k+1}+L_{k+1}\left(I+\beta_1 L_{k+1}^{\mathsf{T}}L_{k+1}\right)^{-1}L_{k+1}^{\mathsf{T}}\right)^{-1} \times L_{k+1}\left(I+\beta_1 L_{k+1}^{\mathsf{T}}L_{k+1}\right)^{-1}L_{k+1}^{\mathsf{T}} + 2\left(M_{k+1}+L_{k+1}\left(I+\beta_1 L_{k+1}^{\mathsf{T}}L_{k+1}\right)^{-1}L_{k+1}^{\mathsf{T}}\right)^{-1} + \beta_1 I-\beta_1^2 L_{k+1}\left(I+\beta_1 L_{k+1}^{\mathsf{T}}L_{k+1}\right)^{-1}L_{k+1}^{\mathsf{T}} \preceq 2(M_{k+1}+\alpha_{1,k+1}L_{k+1}L_{k+1}^{\mathsf{T}})^{-1}+2\beta_1 I \tag{31}$$

where $\alpha_{1,k+1}=\|I+\beta_1 L_{k+1}^{\mathsf{T}}L_{k+1}\|^{-1}$. The equalities $(\dagger)$, $(\ddagger)$, and $(\diamond)$ in (31) are obtained via three successive applications of the Woodbury identity and the inequality $(\diamond)$ in (31) is obtained by using the Young-like inequality

$$(f(v)+g(v))^{\mathsf{T}}(f(v)+g(v))\leq 2f^{\mathsf{T}}(v)g(v)+2\,g^{\mathsf{T}}(v)f(v) \tag{32}$$

with $f(v)=(M_{k+1}+L_{k+1}(I+\beta_1 L_{k+1}^{\mathsf{T}}L_{k+1})^{-1}L_{k+1}^{\mathsf{T}})^{-\frac{1}{2}}v$ and $g(v)=-\beta_1(M_{k+1}+L_{k+1}(I+\beta_1 L_{k+1}^{\mathsf{T}}L_{k+1})^{-1}L_{k+1}^{\mathsf{T}})^{-\frac{1}{2}} L_{k+1}(I+\beta_1 L_{k+1}^{\mathsf{T}}L_{k+1})^{-1}L_{k+1}^{\mathsf{T}}v$.

Plugging in the value of M_{k+1} from the update equations (17), we have

$$\left(P_{k+1}+L_{k+1}L_{k+1}^{\mathsf{T}}\right)^{-1}\preceq 2\beta_1 I+2\tilde{A}_{\mathfrak{v}}^{-\mathsf{T}} \times\left(P_k+\tilde{A}_{\mathfrak{v}}^{-1}\left(\tilde{G}_{\mathfrak{v}}Q_k\tilde{G}_{\mathfrak{v}}^{\mathsf{T}}+\alpha_{1,k+1}L_{k+1}L_{k+1}^{\mathsf{T}}\right)\tilde{A}_{\mathfrak{v}}^{-\mathsf{T}}\right)^{-1}\tilde{A}_{\mathfrak{v}}^{-1}. \tag{33}$$

Now, for any $k\geq 0$, define recursively

$$L_jL_j^{\mathsf{T}}=\tilde{A}_{\mathfrak{v}}^{-1}\left(\tilde{G}_{\mathfrak{v}}Q_j\tilde{G}_{\mathfrak{v}}^{\mathsf{T}}+\alpha_{1,j+1}L_{j+1}L_{j+1}^{\mathsf{T}}\right)\tilde{A}_{\mathfrak{v}}^{-\mathsf{T}} \tag{34}$$

for $k\leq j\leq k+N_c-1$, with $L_{k+N_c}L_{k+N_c}^{\mathsf{T}}=0$. By substituting (34) into (33), and repeatedly applying the resulting inequality we obtain

$$P_{k+N_c}^{-1}\preceq 2^{N_c}\Phi^{-\mathsf{T}}(k+N_c,k)\left(P_k+L_kL_k^{\mathsf{T}}\right)^{-1} \times\Phi^{-1}(k+N_c,k)+2\beta_1\sum_{i=0}^{N_c-1}2^i \times\Phi^{-\mathsf{T}}(k+N_c,k+N_c-i)\,\Phi^{-1}(k+N_c,k+N_c-i). \tag{35}$$

Using the bounds defined in Assumption 5, (20), and (34), we can write

$$L_kL_k^{\mathsf{T}}\succeq\gamma_1\Phi^{-1}(k+N_c,k)W_c(k+N_c,k)\Phi^{-\mathsf{T}}(k+N_c,k) \tag{36}$$

with $\gamma_1=\underline{\vartheta}\prod_{j=k}^{k+N_c-1}\alpha_{1,j+1}$ [41]. Aggregating the bounds in (35), (36), and invoking Assumptions 2 and 3, we have

$$P_{k+N_c}\succeq\underbrace{\left(\frac{2^{N_c}}{\gamma_1\delta}+2\beta_1\sum\nolimits_{i=0}^{N_c-1}\left(\frac{2}{\underline{\alpha}}\right)^i\right)^{-1}}_{\underline{\pi}(N_c)}I. \tag{37}$$

Proof of Lemma 2: Suppose Y_{k+1} is an arbitrary matrix. We can write

$$(P_{k+1}^{-1}+Y_{k+1}^{\mathsf{T}}Y_{k+1})^{-1}=\left(\left(\tilde{A}_{\mathfrak{v}}P_k\tilde{A}_{\mathfrak{v}}^{\mathsf{T}}+\tilde{G}_{\mathfrak{v}}Q_k\tilde{G}_{\mathfrak{v}}^{\mathsf{T}}\right)^{-1}+Z_{k+1}^{\mathsf{T}}Z_{k+1}\right)^{-1} \tag{38}$$

where the matrix Z_{k+1} is defined as

$$Z_{k+1}=C_{k+1}^{\mathsf{T}}R_{k+1}^{-1}C_{k+1}+Y_{k+1}^{\mathsf{T}}Y_{k+1}. \tag{39}$$

Using the bounds in Assumptions 2 and 5, and defining $\beta_2=\beta\overline{\vartheta}$, we have

$$\begin{aligned}&\left(P_{k+1}^{-1}+Y_{k+1}^{\mathsf{T}}Y_{k+1}\right)^{-1}\\ &\preceq\left(\left(\tilde{A}_{\mathfrak{v}}P_k\tilde{A}_{\mathfrak{v}}^{\mathsf{T}}+\beta_2 I\right)^{-1}+Z_{k+1}^{\mathsf{T}}Z_{k+1}\right)^{-1}\\ &\overset{(\triangle)}{=}\left(\frac{1}{\beta_2}I-\frac{1}{\beta_2^2}\tilde{A}_{\mathfrak{v}}\left(P_k^{-1}+\frac{1}{\beta_2}\tilde{A}_{\mathfrak{v}}^{\mathsf{T}}\tilde{A}_{\mathfrak{v}}\right)^{-1}\tilde{A}_{\mathfrak{v}}^{\mathsf{T}}+Z_{k+1}^{\mathsf{T}}Z_{k+1}\right)^{-1}\\ &\overset{(\triangledown)}{=}\frac{1}{\beta_2^2}\left(\frac{1}{\beta_2}I+Z_{k+1}^{\mathsf{T}}Z_{k+1}\right)^{-1}\tilde{A}_{\mathfrak{v}} \times\left(P_k^{-1}+\frac{1}{\beta_2}\tilde{A}_{\mathfrak{v}}^{\mathsf{T}}\tilde{A}_{\mathfrak{v}}-\frac{1}{\beta_2^2}\tilde{A}_{\mathfrak{v}}^{\mathsf{T}}\left(\frac{1}{\beta_2}I+Z_{k+1}^{\mathsf{T}}Z_{k+1}\right)^{-1}\tilde{A}_{\mathfrak{v}}\right)^{-1} \times\tilde{A}_{\mathfrak{v}}^{\mathsf{T}}\left(\frac{1}{\beta_2}I+Z_{k+1}^{\mathsf{T}}Z_{k+1}\right)^{-1}+\left(\frac{1}{\beta_2}I+Z_{k+1}^{\mathsf{T}}Z_{k+1}\right)^{-1}\\ &\overset{(\cdot)}{=}\frac{1}{\beta_2^2}\left(\beta_2 I-\beta_2^2 Z_{k+1}^{\mathsf{T}}\left(I+\beta_2 Z_{k+1}Z_{k+1}^{\mathsf{T}}\right)^{-1}Z_{k+1}\right)\tilde{A}_{\mathfrak{v}} \times\left(P_k^{-1}+\tilde{A}_{\mathfrak{v}}^{\mathsf{T}}Z_{k+1}^{\mathsf{T}}\left(I+\beta_2 Z_{k+1}Z_{k+1}^{\mathsf{T}}\right)^{-1}Z_{k+1}\tilde{A}_{\mathfrak{v}}\right)^{-1}\tilde{A}_{\mathfrak{v}}^{\mathsf{T}} \times\left(\beta_2 I-\beta_2^2 Z_{k+1}^{\mathsf{T}}\left(I+\beta_2 Z_{k+1}Z_{k+1}^{\mathsf{T}}\right)^{-1}Z_{k+1}\right) +\beta_2 I-\beta_2^2 Z_{k+1}^{\mathsf{T}}\left(I+\beta_2 Z_{k+1}Z_{k+1}^{\mathsf{T}}\right)^{-1}Z_{k+1}\\ &\overset{(\cdot\cdot)}{\preceq}2\beta_2^2 Z_{k+1}^{\mathsf{T}}\left(I+\beta_2 Z_{k+1}Z_{k+1}^{\mathsf{T}}\right)^{-1}Z_{k+1}\tilde{A}_{\mathfrak{v}} \times\left(P_k^{-1}+\tilde{A}_{\mathfrak{v}}^{\mathsf{T}}Z_{k+1}^{\mathsf{T}}\left(I+\beta_2 Z_{k+1}Z_{k+1}^{\mathsf{T}}\right)^{-1}Z_{k+1}\tilde{A}_{\mathfrak{v}}\right)^{-1} \times\tilde{A}_{\mathfrak{v}}^{\mathsf{T}}Z_{k+1}^{\mathsf{T}}\left(I+\beta_2 Z_{k+1}Z_{k+1}^{\mathsf{T}}\right)^{-1}Z_{k+1} +2\tilde{A}_{\mathfrak{v}}\left(P_k^{-1}+\tilde{A}_{\mathfrak{v}}^{\mathsf{T}}Z_{k+1}^{\mathsf{T}}\left(I+\beta_2 Z_{k+1}Z_{k+1}^{\mathsf{T}}\right)^{-1}Z_{k+1}\tilde{A}_{\mathfrak{v}}\right)^{-1}\tilde{A}_{\mathfrak{v}}^{\mathsf{T}} +\beta_2 I-\beta_2^2 Z_{k+1}^{\mathsf{T}}\left(I+\beta_2 Z_{k+1}Z_{k+1}^{\mathsf{T}}\right)^{-1}Z_{k+1}\\ &\preceq 2\tilde{A}_{\mathfrak{v}}(P_k^{-1}+\alpha_{2,k+1}\tilde{A}_{\mathfrak{v}}^{\mathsf{T}}Z_{k+1}^{\mathsf{T}}Z_{k+1}Z_{k+1}\tilde{A}_{\mathfrak{v}})^{-1}+2\beta_2 I\end{aligned} \tag{40}$$

where $\alpha_{2,k+1}=\|I+\beta_2 Z_{k+1}Z_{k+1}^{\mathsf{T}}\|^{-1}$. The equalities $(\triangle)$, $(\triangledown)$, and $(\cdot)$ in (40) are obtained via three successive applications of the Woodbury identity and the inequality $(\cdot\cdot)$ in (40) is obtained by using the Young-like inequality (32).

Now, for any $k \geq 0$, define

$$Y_j^{\mathsf{T}} Y_j = \alpha_{2,j+1} \tilde{A}_{\mathfrak{v}}^{\mathsf{T}} Z_{j+1}^{\mathsf{T}} Z_{j+1} \tilde{A}_{\mathfrak{v}} \tag{41}$$

where $k \leq j \leq k + N_o - 1$, with $Y_{k+N_o}^{\mathsf{T}} Y_{k+N_o} = 0$. By repeatedly applying (40) and (41), we obtain

$$\begin{aligned} P_{k+N_o} &\preceq 2^{N_o} \Phi\left(k+N_o, k\right) \left(P_k^{-1} + Y_k^{\mathsf{T}} Y_k\right)^{-1} \\ &\times \Phi^{\mathsf{T}}\left(k+N_o, k\right) + 2\beta_2 \sum_{i=0}^{N_o-1} 2^i \\ &\times \Phi\left(k+N_o, k+N_o-i\right) \Phi^{\mathsf{T}}\left(k+N_o, k+N_o-i\right). \end{aligned} \tag{42}$$

Aggregating the bounds in Assumption 5, (21), (39), and (41), we have

$$Y_k^{\mathsf{T}} Y_k \succeq \gamma_2 W_o(k+N_o, k) \tag{43}$$

with $\gamma_2 = \frac{1}{\overline{\rho}} \prod_{j=k}^{k+N_o-1} \alpha_{2,j+1}$ [41]. Finally, we assimilate the inequalities in (42) and (43), along with Assumptions 2 and 4, which gives us

$$P_{k+N_o} \preceq \underbrace{\left(\frac{2^{N_o}}{\gamma_2 \varepsilon} + 2\beta_2 \sum\nolimits_{i=0}^{N_o-1} \left(2\overline{\alpha}\right)^i\right)}_{\overline{\pi}(N_o)} I. \tag{44}$$

■

Proof: *Proof of Theorem 2*: From the equations (11a) and (16), we can obtain the dynamics of the estimation error $e[k]$, which admits the following form:

$$\begin{aligned} e[k+1] &= \left(I - K_{k+1} C_{k+1}\right) \left(\tilde{A}_{\mathfrak{v}} e[k] - \tilde{G}_{\mathfrak{v}} r[k]\right) \\ &+ K_{k+1} v[k+1]. \end{aligned} \tag{45}$$

In order to prove exponential input-to-state stability of the estimation error, we consider the candidate Lyapunov function

$$V_k = e[k]^{\mathsf{T}} P_k^{-1} e[k]. \tag{46}$$

Consider any time index k that satisfies $k \geq \max\{N_c, N_o\}$ and let S_{k+1} be an arbitrary matrix. We have

$$\begin{aligned} &e[k+1]^{\mathsf{T}} \left(P_{k+1} + S_{k+1} S_{k+1}^{\mathsf{T}}\right)^{-1} e[k+1] \\ &= \left(\tilde{A}_{\mathfrak{v}} e[k] - \tilde{G}_{\mathfrak{v}} r[k]\right)^{\mathsf{T}} M_{k+1}^{-1} \left(\tilde{A}_{\mathfrak{v}} e[k] - \tilde{G}_{\mathfrak{v}} r[k]\right) \\ &+ v[k+1]^{\mathsf{T}} R_{k+1}^{-1} v[k+1] \\ &- \left(C_{k+1}\left(\tilde{A}_{\mathfrak{v}} e[k] - \tilde{G}_{\mathfrak{v}} r[k]\right) - v[k+1]\right)^{\mathsf{T}} \\ &\times \left(C_{k+1} M_{k+1} C_{k+1}^{\mathsf{T}} + R_{k+1}\right)^{-1} \\ &\times \left(C_{k+1}\left(\tilde{A}_{\mathfrak{v}} e[k] - \tilde{G}_{\mathfrak{v}} r[k]\right) - v[k+1]\right) \\ &- \left(M_{k+1}^{-1}\left(\tilde{A}_{\mathfrak{v}} e[k] - \tilde{G}_{\mathfrak{v}} r[k]\right) + C_{k+1}^{\mathsf{T}} R_{k+1}^{-1} v[k+1]\right)^{\mathsf{T}} S_{k+1} \\ &\times \left(I + S_{k+1}^{\mathsf{T}}\left(M_{k+1}^{-1} + C_{k+1}^{\mathsf{T}} R_{k+1}^{-1} C_{k+1}\right) S_{k+1}\right)^{-1} S_{k+1}^{\mathsf{T}} \\ &\times \left(M_{k+1}^{-1}\left(\tilde{A}_{\mathfrak{v}} e[k] - \tilde{G}_{\mathfrak{v}} r[k]\right) + C_{k+1}^{\mathsf{T}} R_{k+1}^{-1} v[k+1]\right) \\ &\overset{(\bullet)}{\leq} \left(\tilde{A}_{\mathfrak{v}} e[k] - \tilde{G}_{\mathfrak{v}} r[k]\right)^{\mathsf{T}} M_{k+1}^{-1} \left(\tilde{A}_{\mathfrak{v}} e[k] - \tilde{G}_{\mathfrak{v}} r[k]\right) \\ &+ 2v[k+1]^{\mathsf{T}} R_{k+1}^{-1} v[k+1] - \frac{1}{2}\left(\tilde{A}_{\mathfrak{v}} e[k] - \tilde{G}_{\mathfrak{v}} r[k]\right)^{\mathsf{T}} \\ &\times M_{k+1}^{-1} S_{k+1} \left(I + S_{k+1}^{\mathsf{T}}\left(M_{k+1}^{-1} + C_{k+1}^{\mathsf{T}} R_{k+1}^{-1} C_{k+1}\right) S_{k+1}\right)^{-1} \\ &\times S_{k+1}^{\mathsf{T}} M_{k+1}^{-1} \left(\tilde{A}_{\mathfrak{v}} e[k] - \tilde{G}_{\mathfrak{v}} r[k]\right) \\ &\overset{(\bullet\bullet)}{\leq} \left(1 - \frac{\alpha_{3,k+1}}{2}\right) \left(\tilde{A}_{\mathfrak{v}} e[k] - \tilde{G}_{\mathfrak{v}} r[k]\right)^{\mathsf{T}} M_{k+1}^{-1} \\ &\times \left(\tilde{A}_{\mathfrak{v}} e[k] - \tilde{G}_{\mathfrak{v}} r[k]\right) + \frac{\alpha_{3,k+1}}{2} \left(\tilde{A}_{\mathfrak{v}} e[k] - \tilde{G}_{\mathfrak{v}} r[k]\right)^{\mathsf{T}} \\ &\times \left(M_{k+1} + S_{k+1} S_{k+1}^{\mathsf{T}}\right)^{-1} \left(\tilde{A}_{\mathfrak{v}} e[k] - \tilde{G}_{\mathfrak{v}} r[k]\right) \\ &+ 2v[k+1]^{\mathsf{T}} R_{k+1}^{-1} v[k+1] \\ &\overset{(\square)}{\leq} \left(1 - \frac{\alpha_{3,k+1}}{2}\right)(1+\varepsilon_3)\, e[k]^{\mathsf{T}} P_k^{-1} e[k] \\ &+ \frac{\alpha_{3,k+1}}{2}(1+\varepsilon_3)\, e[k]^{\mathsf{T}} \\ &\times \left(P_k + \tilde{A}_{\mathfrak{v}}^{-1}\left(\tilde{G}_{\mathfrak{v}} Q_k \tilde{G}_{\mathfrak{v}}^{\mathsf{T}} + S_{k+1} S_{k+1}^{\mathsf{T}}\right) \tilde{A}_{\mathfrak{v}}^{-\mathsf{T}}\right)^{-1} e[k] \\ &+ \left(\frac{1+\varepsilon_3}{\varepsilon_3}\right) r[k]^{\mathsf{T}} Q_k^{-1} r[k] + 2v[k+1]^{\mathsf{T}} R_{k+1}^{-1} v[k+1] \end{aligned} \tag{47}$$

with $\alpha_{3,k+1} = \|I + \frac{1}{\pi} S_{k+1}^{\mathsf{T}} S_{k+1}\|^{-1}$ and $\varepsilon_3 \in \mathbb{R}^+$. The inequality $(\bullet)$ in (47) is a consequence of the Young-like inequality (32), the inequality $(\bullet\bullet)$ in (47) results from the Woodbury identity used in conjunction with Lemma 1 and (30), whereas the inequality $(\square)$ is a result of (17) and (32).

From Assumption 5 and (47), we can write

$$\begin{aligned} e[k+1]^{\mathsf{T}} P_{k+1}^{-1} e[k+1] &\leq (1+\varepsilon_3) e[k]^{\mathsf{T}} P_k^{-1} e[k] \\ &+ \left(\frac{1+\varepsilon_3}{\varepsilon_3 \underline{\vartheta}}\right) \|r[k]\|^2 + \left(\frac{2}{\underline{\rho}}\right) \|v[k+1]\|^2. \end{aligned} \tag{48}$$

Now, from the equality

$$S_k S_k^{\mathsf{T}} = \tilde{A}_{\mathfrak{v}}^{-1} \left(\tilde{G}_{\mathfrak{v}} Q_k \tilde{G}_{\mathfrak{v}}^{\mathsf{T}} + S_{k+1} S_{k+1}^{\mathsf{T}}\right) \tilde{A}_{\mathfrak{v}}^{-\mathsf{T}} \tag{49}$$

we have

$$\begin{aligned} &e[k+1]^{\mathsf{T}} \left(P_{k+1} + S_{k+1} S_{k+1}^{\mathsf{T}}\right)^{-1} e[k+1] \\ &\leq \left(\frac{1+\varepsilon_3}{\varepsilon_3 \underline{\vartheta}}\right) \|r[k]\|^2 + \left(1 - \frac{\alpha_{3,k+1}}{2}\right)(1+\varepsilon_3)\, e[k]^{\mathsf{T}} P_k^{-1} e[k] \\ &+ \left(\frac{2}{\underline{\rho}}\right) \|v[k+1]\|^2 \\ &+ \frac{\alpha_{3,k+1}}{2}(1+\varepsilon_3) e[k]^{\mathsf{T}} \left(P_k + S_k S_k^{\mathsf{T}}\right)^{-1} e[k]. \end{aligned} \tag{50}$$

We let $S_{k+N_c} S_{k+N_c}^{\mathsf{T}} = 0$ and by repeated application of (50), we get

$$e[k+N_c]^{\mathsf{T}} P_{k+N_c}^{-1} e[k+N_c]$$

$$\leq (1-\gamma_3)(1+\varepsilon_3)^{N_c} e[k]^{\mathsf{T}} P_k^{-1} e[k] + \gamma_3 (1+\varepsilon_3)^{N_c} e[k]^{\mathsf{T}} \left(P_k + S_k S_k^{\mathsf{T}}\right)^{-1} e[k] + \frac{(1+\varepsilon_3)^{N_c}}{\varepsilon_3 \underline{\vartheta}} \sum_{i=k}^{k+N_c-1} \|r[i]\|^2 + \frac{2(1+\varepsilon_3)^{N_c-1}}{\underline{\rho}} \sum_{j=k}^{k+N_c-1} \|v[j+1]\|^2 \quad (51)$$

where $\gamma_3 = \frac{1}{2^{N_c}} \prod_{i=k}^{k+N_c-1} \alpha_{3,i+1}$. Using the recursive definition in (49), the bounds in (20), and Assumption 5, we get the bound

$$S_k S_k^{\mathsf{T}} \succeq \underline{\vartheta} \Phi^{-1}(k+N_c,k) W_c(k+N_c,k) \Phi^{-\mathsf{T}}(k+N_c,k). \quad (52)$$

With the inequality (52), we can then aggregate the bounds in Assumptions 2 and 3 and Lemma 2 to then obtain

$$S_k S_k^{\mathsf{T}} \succeq \frac{\underline{\vartheta}\delta}{\overline{\alpha}^{N_c}\overline{\pi}} P_k. \quad (53)$$

Now, given the Lyapunov function $V_k = e[k]^{\mathsf{T}} P_k^{-1} e[k]$ and the bound in (48), we have

$$V_k \leq (1+\varepsilon_3)^{k-k_0} V_{k_0} + \frac{(1+\varepsilon_3)^{k-k_0}}{\varepsilon_3 \underline{\vartheta}} \sum_{i=k_0}^{k-1} \|r[i]\|^2 + \frac{2(1+\varepsilon_3)^{k-k_0-1}}{\underline{\rho}} \sum_{j=k_0}^{k-1} \|v[j+1]\|^2 \quad (54)$$

for all $k \geq k_0 \geq \max\{N_c, N_o\}$. Using Assumption 5, (51), and (53), we have

$$V_{k+N_c} \leq \eta_3 V_k + \frac{(1+\varepsilon_3)^{N_c}}{\varepsilon_3 \underline{\vartheta}} \sum_{i=k}^{k+N_c-1} \|r[i]\|^2 + \frac{2(1+\varepsilon_3)^{N_c-1}}{\underline{\rho}} \sum_{j=k}^{k+N_c-1} \|v[j+1]\|^2 \quad (55)$$

for all $k \geq k_0 \geq \max\{N_c, N_o\}$ and with

$$\eta_3 = \left(1 - \frac{\gamma_3 \underline{\vartheta}\delta}{\underline{\vartheta}\delta + \overline{\alpha}^{N_c}\overline{\pi}}\right)(1+\varepsilon_3)^{N_c}. \quad (56)$$

If we assume, without loss of generality, that ε_3 is chosen such that $\eta_3 < 1$, then from (54) and (55), we obtain

$$V_k \leq \left(\frac{(1+\varepsilon_3)^{N_c}}{\eta_3}\right)^{\frac{N_c-1}{N_c}} \eta_3^{\frac{k-k_0}{N_c}} V_{k_0} + \frac{N_c (1+\varepsilon_3)^{N_c}}{\varepsilon_3 \underline{\vartheta} (1-\eta_3)} \max_{k_0 \leq i \leq k-1} \|r[i]\|^2 + \frac{2N_c (1+\varepsilon_3)^{N_c-1}}{\underline{\rho}(1-\eta_3)} \max_{k_0 \leq j \leq k-1} \|v[j+1]\|^2 \quad (57)$$

for all $k \geq k_0 \geq \max\{N_c, N_o\}$.

On the other hand, from Lemmas 1 and 2, we have the following bounds on the Lyapunov function

$$\frac{1}{\overline{\pi}} \|e[k]\|^2 \leq V_k \leq \frac{1}{\underline{\pi}} \|e[k]\|^2 \quad (58)$$

for all $k \geq \max\{N_c, N_o\}$ [41].

Thus, using (57) and (58), the proof of the theorem follows with

$$\sigma = \sqrt{\frac{3\overline{\pi}}{\underline{\pi}}} \left(\frac{(1+\varepsilon_3)^{N_c}}{\eta_3}\right)^{\frac{N_c-1}{2N_c}} \quad (59a)$$

$$\tau = \eta_3^{\frac{1}{2N_c}} \quad (59b)$$

$$\chi = \sqrt{\frac{3\overline{\pi} N_c (1+\varepsilon_3)^{N_c}}{\varepsilon_3 \underline{\vartheta}(1-\eta_3)}} \quad (59c)$$

and

$$\psi = \sqrt{\frac{6\overline{\pi} N_c (1+\varepsilon_3)^{N_c-1}}{\underline{\rho}(1-\eta_3)}}. \quad (59d)$$

■

REFERENCES

[1] F. C. Moon, *Chaotic and Fractal Dynamics: Introduction for Applied Scientists and Engineers*. Hoboken, NJ, USA: Wiley, 2008.

[2] B. N. Lundstrom, M. H. Higgs, W. J. Spain, and A. L. Fairhall, "Fractional differentiation by neocortical pyramidal neurons," *Nature Neurosci.*, vol. 11, no. 11, 2008, Art. no. 1335.

[3] G. Werner, "Fractals in the nervous system: Conceptual implications for theoretical neuroscience," *Front. Physiol.*, vol. 1, Jul. 2010, Art. no. 15.

[4] R. G. Turcott and M. C. Teich, "Fractal character of the electrocardiogram: Distinguishing heart-failure and normal patients," *Ann. Biomed. Eng.*, vol. 24, no. 2, pp. 269–293, 1996.

[5] S. Thurner, C. Windischberger, E. Moser, P. Walla, and M. Barth, "Scaling laws and persistence in human brain activity," *Physica A: Stat. Mechan. Appl.*, vol. 326, no. 3–4, pp. 511–521, 2003.

[6] M. C. Teich, C. Heneghan, S. B. Lowen, T. Ozaki, and E. Kaplan, "Fractal character of the neural spike train in the visual system of the cat," *J. Opt. Soc. Amer.*, vol. 14, no. 3, pp. 529–546, 1997.

[7] B. J. West, M. Turalska, and P. Grigolini, *Networks of Echoes: Imitation, Innovation and Invisible Leaders*. Berlin, Germany: Springer, 2014.

[8] Y. Cao, Y. Li, W. Ren, and Y. Chen, "Distributed coordination of networked fractional-order systems," *IEEE Trans. Syst., Man, Cybern., Part B*, vol. 40, no. 2, pp. 362–370, Apr. 2010.

[9] Y. Chen, "Fractional calculus, delay dynamics and networked control systems," in *Proc. 3rd Int. Symp. Resilient Control Syst.*, 2010, pp. 58–63.

[10] W. Ren and Y. Cao, *Distributed Coordination of Multi-Agent Networks: Emergent Problems, Models, and Issues*, vol. 1. Berlin, Germany: Springer, 2011.

[11] Y. Xue, S. Rodriguez, and P. Bogdan, "A spatio-temporal fractal model for a CPS approach to brain-machine-body interfaces," in *Proc. Design, Automat. Test Eur. Conf. Exhib.*, 2016, pp. 642–647.

[12] S. Chatterjee, O. Romero, A. Ashourvan, and S. Pequito, "Fractional-order model predictive control as a framework for electrical neurostimulation in epilepsy," *J. Neural Eng.*, vol. 17, no. 6, 2020, Art. no. 066017.

[13] R. L. Magin, *Fractional Calculus in Bioengineering*. Redding, CT, USA: Begell House, 2006.

[14] J. Sabatier, C. Farges, M. Merveillaut, and L. Feneteau, "On observability and pseudo state estimation of fractional order systems," *Eur. J. Control*, vol. 18, no. 3, pp. 260–271, 2012.

[15] D. Sierociuk and A. Dzieliński, "Fractional Kalman filter algorithm for the states, parameters and order of fractional system estimation," *Int. J. Appl. Math. Comput. Sci.*, vol. 16, pp. 129–140, 2006.

[16] B. Safarinejadian, N. Kianpour, and M. Asad, "State estimation in fractional-order systems with coloured measurement noise," *Trans. Inst. Meas. Control*, vol. 40, no. 6, pp. 1819–1835, 2018.

[17] B. Safarinejadian, M. Asad, and M. S. Sadeghi, "Simultaneous state estimation and parameter identification in linear fractional order systems using coloured measurement noise," *Int. J. Control*, vol. 89, no. 11, pp. 2277–2296, 2016.
[18] N. Miljković, N. Popović, O. Djordjević, L. Konstantinović, and T. B. šekara, "ECG artifact cancellation in surface EMG signals by fractional order calculus application," *Comput. Meth. Programs Biomed.*, vol. 140, pp. 259–264, 2017.
[19] S. Najar, M. N. Abdelkrim, M. Abdelhamid, and A. Mohamed, "Discrete fractional Kalman filter," *IFAC Proc. Vol.*, vol. 42, no. 19, pp. 520–525, 2009.
[20] S. Chatterjee and S. Pequito, "Dealing with state estimation in fractional-order systems under artifacts," in *Proc. Amer. Control Conf.*, 2019, pp. 878–883.
[21] Z. Gao, "Fractional-order Kalman filters for continuous-time linear and nonlinear fractional-order systems using Tustin generating function," *Int. J. Control*, vol. 92, no. 5, pp. 960–974, 2019.
[22] X. Huang, Z. Gao, C. Yang, and F. Liu, "State estimation of continuous-time linear fractional-order systems disturbed by correlated colored noises via Tustin generating function," *IEEE Access*, vol. 8, pp. 18362–18373, 2020.
[23] J. W. Britton et al., "Electroencephalography (EEG): An introductory text and atlas of normal and abnormal findings in adults, children, and infants," Chicago, IL, USA: American Epilepsy Society, 2016.
[24] R. E. Mortensen, "Maximum-likelihood recursive nonlinear filtering," *J. Optim. Theory Appl.*, vol. 2, no. 6, pp. 386–394, 1968.
[25] O. Hijab, "Minimum energy estimation," Ph.D. dissertation, Dept. Math., Univ. California, Berkeley, CA, USA, 1980.
[26] W. H. Fleming, "Deterministic nonlinear filtering," *Annali dellaScuolaNormaleSuperiore di Pisa-Classe di Scienze*, vol. 25, no. 3–4, pp. 435–454, 1997.
[27] J. C. Willems, "Deterministic Kalman filtering," *J. Econometrics*, vol. 118, no. 1.2, pp. 341–373, Jan./Feb. 2004.
[28] D. Buchstaller, J. Liu, and M. French, "The deterministic interpretation of the Kalman filter," *Int. J. Control*, vol. 9, pp. 3226–3236, 2020.
[29] P. Swerling, "Modern state estimation methods from the viewpoint of the method of least squares," *IEEE Trans. Autom. Control*, vol. AC-16, no. 6, pp. 707–719, Dec. 1971.
[30] S. Bonnabel and J.-J. Slotine, "A contraction theory-based analysis of the stability of the deterministic extended Kalman filter," *IEEE Trans. Autom. Control*, vol. 60, no. 2, pp. 565–569, Feb. 2015.
[31] F. Fagnani and J. C. Willems, "Deterministic Kalman filtering in a behavioral framework," *Syst. Control Lett.*, vol. 32, no. 5, pp. 301–312, 1997.
[32] A. J. Krener, "The convergence of the minimum energy estimator," in *New Trends in Nonlinear Dynamics and Control and Their Applications*. Berlin, Germany: Springer, 2003, pp. 187–208.
[33] A. J. Krener, "Minimum Energy Estimation Applied to the Lorenz Attractor," in *Numerical Methods for Optimal Control Problems*. Berlin, Germany: Springer, 2018, pp. 165–182.
[34] A. P. Aguiar and J. P. Hespanha, "Minimum-energy state estimation for systems with perspective outputs," *IEEE Trans. Autom. Control*, vol. 51, no. 2, pp. 226–241, Feb. 2006.
[35] V. Hassani, A. P. Aguiar, M. Athans, and A. M. Pascoal, "Multiple model adaptive estimation and model identification using a minimum energy criterion," in *Proc. Amer. Control Conf.*, 2009, pp. 518–523.
[36] S. Pequito, A. P. Aguiar, and D. A. Gomes, "The entropy penalized minimum energy estimator," in *Proc. IEEE 48th Conf. Decis. Control Held Jointly With 28th Chinese Control Conf.*, 2009, pp. 1285–1290.
[37] A. Alessandretti, A. P. Aguiar, J. a. P. Hespanha, and P. Valigi, "A minimum energy solution to monocular simultaneous localization and mapping," in *Proc. IEEE 50th Conf. Decis. Control Eur. Control Conf.*, 2011, pp. 4566–4571.
[38] T. N. Ha and A. P. Aguiar, "Cooperative joint estimation and localization using mobile multi-agent systems: A minimum energy estimator approach," in *Proc. Eur. Control Conf.*, 2018, pp. 2224–2229.
[39] M. Zamani, J. Trumpf, and R. Mahony, "Minimum-energy filtering for attitude estimation," *IEEE Trans. Autom. Control*, vol. 58, no. 11, pp. 2917–2921, Nov. 2013.
[40] W. M. McEneaney, "Robust/H_∞ filtering for nonlinear systems," *Syst. Control Lett.*, vol. 33, no. 5, pp. 315–325, 1998.
[41] M. Haring and T. A. Johansen, "On the stability bounds of Kalman filters for linear deterministic discrete-time systems," *IEEE Trans. Autom. Control*, vol. 65, no. 10, pp. 4434–4439, Oct. 2020.
[42] D. Baleanu, K. Diethelm, E. Scalas, and J. J. Trujillo, *Fractional Calculus: Models and Numerical Methods*, vol. 3. Singapore: World Scientific, 2012.
[43] G. E. Andrews, R. Askey, and R. Roy, *Special Functions* (Encyclopedia of Mathematics and its Applications Series). Cambridge, U.K.: Cambridge Univ. Press, 1999.
[44] A. Alessandretti, S. Pequito, G. J. Pappas, and A. P. Aguiar, "Finite-dimensional control of linear discrete-time fractional-order systems," *Automatica*, vol. 115, 2020, Art. no. 108512.
[45] P. Sopasakis and H. Sarimveis, "Stabilising model predictive control for discrete-time fractional-order systems," *Automatica*, vol. 75, pp. 24–31, 2017.
[46] R. E. Kalman, "A new approach to linear filtering and prediction problems," *J. Basic Eng.*, vol. 82, no. 1, pp. 35–45, 031960.
[47] A. A. Stoorvogel and A. Saberi, "The discrete algebraic Riccati equation and linear matrix inequality," *Linear Algebra Appl.*, vol. 274, no. 1–3, pp. 317–365, 1998.
[48] J. P. Hespanha, *Linear Systems Theory*. Princeton, NJ, USA: Princeton Univ. Press, 2018.
[49] D. Nešić and A. Loría, "On uniform asymptotic stability of time-varying parameterized discrete-time cascades," *IEEE Trans. Autom. Control*, vol. 49, no. 6, pp. 875–887, Jun. 2004.
[50] S. Dashkovskiy, B. S. Rüffer, and F. R. Wirth, "An ISS small gain theorem for general networks," *Math. Control, Signals, Syst.*, vol. 19, no. 2, pp. 93–122, 2007.
[51] G. Schalk, D. J. McFarland, T. Hinterberger, N. Birbaumer, and J. R. Wolpaw, "BCI2000: A general-purpose brain-computer interface () system," *IEEE Trans. Biomed. Eng.*, vol. 51, no. 6, pp. 1034–1043, Jun. 2004.
[52] A. L. Goldberger et al., "PhysioBank, PhysioToolkit, and PhysioNet: Components of a new research resource for complex physiologic signals," *Circulation*, vol. 101, no. 23, pp. e215–e220, 2000.
[53] G. Gupta, S. Pequito, and P. Bogdan, "Dealing with unknown unknowns: Identification and selection of minimal sensing for fractional dynamics with unknown inputs," in *Proc. Amer. Control Conf.*, 2018, pp. 2814–2820.
[54] S. Chatterjee and S. Pequito, "On learning discrete-time fractional-order dynamical systems," in *Proc. Amer. Control Conf.*, to be published.
[55] K. B. Petersen and M. S. Pedersen, "The matrix cookbook," Tech. Univ. Denmark, Nov. 2008, version 20121115. [Online]. Available: http://www2.compute.dtu.dk/pubdb/edoc/imm3274.pdf

Sarthak Chatterjee received the bachelor of engineering degree in electronics and telecommunication engineering from Jadavpur University, Kolkata, India, in 2015 and the M.S. and Ph.D. degrees in computer and systems engineering from Rensselaer Polytechnic Institute, Troy, NY, USA, in 2018 and 2021, respectively.

Since 2021, he has been an Associate Scientist – Postdoctoral Fellow with the Global Digital Analytics and Technologies (GDAT) group within Translational Medicine at Merck and Co., Inc., Rahway, NJ, USA. He has also held research internship positions with the Bosch Center for Artificial Intelligence (BCAI), Pittsburgh, PA, USA, and with the School of Electrical and Electronic Engineering, Nanyang Technological University, Singapore. At present, he is interested in data science and digital and healthcare analytics, particularly in the modeling and analysis of streaming data from digital devices in order to develop novel digital biomarkers for Parkinson's disease. His research interests include control theory and mathematical optimization and the applications of the same in designing neurotechnologies and neuromodulation strategies for the treatment of neurodegenerative disorders such as epilepsy.

Andrea Alessandretti received the bachelor's degree in information engineering and the master's degree in informatics and telecommunication engineering from the University of Perugia, Perugia, Italy, in 2007 and 2010, respectively, and the Ph.D. degree in robotics, control and intelligent systems from the Instituto Superior Técnico (IST), Lisbon, Portugal, and the École Polytechnique Fédérale de Lausanne (EPFL), Lausanne, Switzerland, in 2016.

He is currently the Team Lead of the Mechatronics and Robotics group at Hilti Group, Schaan, Liechtenstein. His research interests include mechatronics and advanced robotics with applications to the construction industry.

Antonio Pedro Aguiar (Senior Member, IEEE) received the Licenciatura, M.S., and Ph.D. degrees in electrical and computer engineering (ECE) from the Instituto Superior Técnico (IST), University of Lisbon, Portugal, in 1994, 1998, and 2002, respectively.

He is currently a Professor with the ECE Department with the Faculty of Engineering, University of Porto (FEUP), Porto, Portugal. His research interests include control systems and robotics with a particular focus on mobile networked cyber-physical systems, motion planning, guidance, navigation, and control of single and multiple cooperative/coordinated autonomous robotic vehicles, nonlinear control and estimation theory, optimization-based and optimal control, networked control, the integration of machine learning with feedback control, and large-scale distributed systems.

Sérgio Pequito (Senior Member, IEEE) received the B.Sc. and M.Sc. degrees in applied mathematics from the Instituto Superior Técnico (IST), University of Lisbon, Portugal, in 2007 and 2009, respectively, and the dual Ph.D. degree in electrical and computer engineering with specialization in control theory from IST and Carnegie Mellon University, Pittsburgh, PA, USA, in 2014.

He is currently an associate professor of automatic control in the Department of Information Technology, Uppsala University, Uppsala, Sweden. His research consists of understanding the global qualitative behavior of large-scale systems from their structural or parametric descriptions and provides a rigorous framework for the design, analysis, optimization, and control of large-scale systems. His research interests include neuroscience and biomedicine, where dynamical systems and control-theoretic tools can be leveraged to develop new analysis tools for brain dynamics towards effective personalized medicine and improving brain–computer and brain–machine–brain interfaces.

Dr. Pequito was the recipient of the 2016 O. Hugo Schuck Award in the Theory Category by the American Automatic Control Council and the Best Student Paper Finalist in the 48th IEEE Conference on Decision and Control (2009).